ELSEVIER

Chemical Engineering Journal 121 (2006) 17–26

Chemical Engineering Journal

www.elsevier.com/locate/cej

Influence of the baffle clearance design on hydrodynamics of a two riser rectangular airlift reactor with inverse internal loop and expanded gas–liquid separator

Peter M. Kilonzo [a], Argyrios Margaritis [a,*], M.A. Bergougnou [a], JunTang Yu [b], Ye Qin [b]

[a] *Department of Chemical & Biochemical Engineering, University of Western Ontario, London, Ont., Canada N6A 5B9*

[b] *Biochemical Engineering Research Institute and State Key Laboratory of Bioreactor Engineering, East China University of Science and Technology, P.O. Box 6666, 130 Meilong Road, Shanghai 200237, China*

Received 31 July 2004; received in revised form 10 April 2006; accepted 3 May 2006

Abstract

The influence of baffle clearance design on the liquid circulating velocity, gas holdup and pressure drop in a two riser rectangular airlift reactor with inverse internal loop and expanded gas–liquid separator was investigated using water and mineralized CMC solutions covering a range of effective viscosity from 0.02 to 0.5 Pa s and surface tension from 0.065 to 0.085 N/m. The gas holdup results in the riser, downcomer, and gas–liquid separator were satisfactorily derived using expressions obtained via dimensional analysis. The separator gas holdup was found to be similar to the total gas holdup in the airlift reactor. The baffle clearances were found to influence the liquid circulation velocity to some degree, with the bottom clearance being the significant design parameter. An attempt was also made to correlate the liquid velocity using empirical equations of the loss coefficient in the baffle top and bottom zones. The calculated and observed liquid circulation velocity agreed well with an error of ±29% for the air–water system.

Keywords: Airlift reactor; Top clearance; Bottom clearance; Gas holdup; Liquid velocity; Pressure drop

1. Introduction

The number of attractive features of airlift reactors have led to increasing usage of these contactors in environmental remediation technology, the chemical process industry and the biotechnology-based manufacture [1,2]. Airlift reactors have an established niche in high-strength activated type treatment of wastewater where the high-oxygen transfer capability, low power requirements and non-mechanical agitation are particular advantages of these systems [3,4]. The gas holdup difference causes liquid circulation flow, which is a characteristic behavior in all airlift reactors. In most cases, gas is also circulated since small bubbles are easily entrained into a downcomer by the liquid downflow. Both gas holdup and liquid circulation velocity parameters govern the oxygen transfer from the gas phase to the liquid phase and the homogeneity of the airlift reactor, respectively [5].

The baffle bottom clearance (spacing between the lower end of the baffle and the base plate of the reactor) determines the rate of liquid and gas circulation through the loop. The distance between the upper end of the baffle and the liquid level (the top clearance) determines the amount of liquid/gas in the gas–liquid separation zone, which is above the riser (draft tube sparged) or downcomer (annulus sparged). The geometry of this region alone determines, to a large extent, the proportion of gas that is recycled through the downcomer. Thus, the design of the baffle clearances of an airlift reactor affects the gas holdup difference between the riser and downcomer; hence, the driving force for liquid circulation is affected. Only limited studies exist in the current literature of the effect of baffle clearance design on hydrodynamic performance characteristics of airlift reactors [6–15].

This work reports on the effects of baffle clearance design, on gas holdup and liquid circulation velocity in a two riser rectangular airlift reactor with inverse internal loop (annulus sparged) and expanded gas–liquid separator. Understanding these hydrodynamics is essential to successful design of airlift reactors for environmental engineering and other applications. Its particularity lies in the fact that it is a two riser airlift reactor. The

* Corresponding author. Tel.: +1 519 661 2146; fax: +1 519 661 4275.
E-mail address: amarg@uwo.ca (A. Margaritis).
URL: http://www.eng.uwo.ca/people/amargaritis/.

1385-8947/$ – see front matter © 2006 Elsevier B.V. All rights reserved.
doi:10.1016/j.cej.2006.05.003

Nomenclature

A	cross-section area (m^2)
ALR	airlift reactor
D	diameter (m)
d_B	bubble diameter (m)
E	gas holdup, dimensionless
f	friction loss coefficient, dimensionless
g	gravitational acceleration ($m\,s^{-2}$)
H	height (m)
h	clearance (m)
K	power law consistency index ($Pa\,s^n$)
L	length (m)
n	power law flow behavior index, dimensionless
P	pressure (Pa)
N	Newton
ΔP	pressure drop (Pa)
S.D.	standard deviation, dimensionless
S.T.D. error	standard error, dimensionless
t	time (s)
Δt	average differential response time (s)
U	gas superficial velocity ($m\,s^{-1}$)
$U_{B\infty}$	free rising velocity of bubbles ($m\,s^{-1}$)
V	volume (m^3)
W	width (m)
We	Weber number, dimensionless
y	coefficient, dimensionless
z	axial distance (m)
Δz	differential height (m)

Greek letters

α	coefficient, dimensionless in pp. 11
β	coefficient, dimensionless in pp. 11
δ	coefficient, dimensionless in pp. 11
η	dynamic viscosity (Pa s)
ρ	density (kg/m^3)
σ_L	liquid surface tension (N/m)

Subscripts

b	bottom
bSP	bottom sparger
B	bubble
c	column
C	circulation
CAL	calculated
d	downcomer
dyn	dynamic
D	dispersion
eff	effective
EXP	experimental
f	friction
FSP	free area of flow in the 'region
g	gas
GL	gas–liquid
h	hydraulic
hyd	hydrostatic
L	liquid
m	mixing
max	maximum
mx	mixture
N	nozzle
o	orifice
r	riser
s	separator
t	top
tC	top contraction
tE	top expansion
T	total
u	roughness
SP	sparger

rectangular shape presents good mixing and better mass transfer performance [9,16–22]. Moreover, this shape was chosen because of its application in wastewater treatment: a third phase can be added to be used as microorganism support. Bigger rectangular plants are easier to build than their cylindrical counter parts [23,24].

2. Experimental

2.1. Reactor

The reactor apparatus for investigating the effect of baffle clearance design on the reactor hydrodynamic performance is shown in Fig. 1. The reactor was constructed of Plexiglas (polymethyl methacrylate). It consisted of five sections: a gas–liquid separator, two risers, a downcomer and a bottom section. Each of the two risers and the downcomer shared an adjustable straight rectangular baffle (0.088 m × 1.056 m) as a central wall. The baffles were fitted to the column walls using a strip of rubber between them and the walls to ensure that no fluid traverses either from the riser into the downcomer and vice versa. The bottom clearance h_b between the baffle bottom and the base plate was varied from 0.01 to 0.1 m by adjusting the vertical position of the baffles on the column walls using stainless steel screws. The dimensions of the riser (s) and the downcomer given in Fig. 1 make the ratio of the cross-sectional area of the downcomer to the one of the risers equal to 1.33. The static gas-free height H_L of the liquid was varied in the range 1.0–1.4 m, giving baffle top clearance h_t in the range of 0–0.30 m for the range of gas velocity used in this study. The aspect ratio ($H_{r/d}/D_h$) of the reactor was 10. This ratio value was based on the riser and downcomer height (neglecting the liquid level in the separator) and the hydraulic diameter (D_h) of the riser and downcomer [25,26].

Two-pair ladder-type air spargers were used consisting of perforated plastic glass pipes of i.d. 0.04 m. The spargers were 0.018 m just above the bottom end of the baffles. A total of 138 sparger holes each of which having diameter $D_o = 4.0\,m \times 10^{-4}$ m and equidistantly spaced were used for air

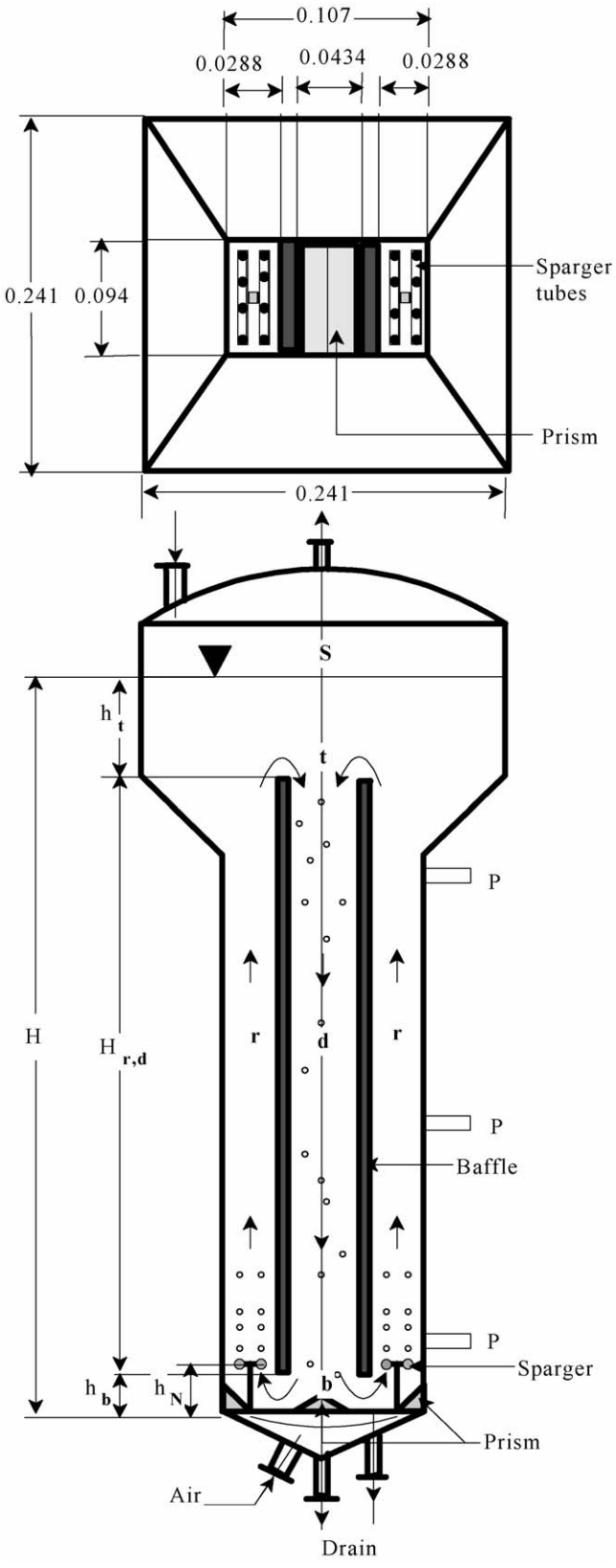

Fig. 1. Dimensioned elevation sketch of rectangular-column airlift reactor used. Symbols: h_t, top clearance; h_b, bottom clearance, h_N sparger clearance; r, riser, d downcomer, s separator, p pressure tap, b bottom, H, height, $H_{r,d}$ riser/downcomer height, t top (all dimensions in m).

distribution, giving a free area of 0.32% of the total cross-section area of the risers. This arrangement gave satisfactory gas distribution over all the orifices of the sparger at the lowest gas flow rates. For the latter, the requirement that the Weber number (W_{eo}):

$$W_{eo} = \frac{U_{og}^2 D_o \rho_{og}}{\sigma_L} > 2 \quad (1)$$

based on the orifice diameter be greater than 2 was satisfied. This was as a result of the small range of flow rates used in this work. Nevertheless, due to the small diameter of the orifices, no weeping was observed even when some of the orifices were not active. The vertical position (h_N) of the spargers above the base plate was allowed to move as the baffle bottom clearance was varied.

Plastic prism inserts placed at the base plate (cf., Fig. 1) eliminated stagnant zones and ensured smooth movement of the fluid from the downcomer into the riser.

2.2. Systems

All experiments were carried out with air. Gas was sparged into the annulus between the column and the riser. Water and mineralized carboxy-methyl cellulose (CMC-Sigma Sodium salt, Medium Viscosity, No. C-4989) aqueous solutions were used as the liquid phase. The physical properties of the experimental media for which the data points were obtained are summarized in Table 1.

Air was sourced from a laboratory compressor via a pressure regulator, needle valve and rotameter that facilitated precise adjustment of gas flow rate. Compressed and oil-free air was used as the gas phase in all experiments. The air superficial velocity was varied from 0.03 to 0.25 m s^{-1}.

2.3. Measurements

The local gas holdups in the riser and the downcomer were determined manometrically [1]. The riser and downcomer each had three manometer/pressure taps located at 0.107 m (bottom port), 0.515 m (middle port) and 0.910 m (top port), respectively, from the base plate and were connected to inverted three-tube type water manometers. For each operating condition, a profile of E_g versus the height Δz in each region could be drawn according to the following expression [8]:

$$E_{gr,d} = 1 - \left(\frac{\Delta P_{r,d}}{\rho_L g \Delta z}\right) \quad (2)$$

Table 1
Properties of experimental media used for data presentation

Medium	Density	Surface tension	Power-law parameters	
	ρ_L (kg/m^3)	σ_L (N/m)	n (–)	K (Pa s^n)
De-ionized water	1000	0.0735	1.000	0.001
0.15 M NaCl–0.25% CMC solution	1004	0.0740	0.902	0.016
0.15 M NaCl–0.5% CMC solution	1007	0.0750	0.864	0.035

The overall gas holdup (E_T) was determined by visual measurements of the clear liquid height (H_L) and the aerated liquid height (H_D) according to the following equation:

$$E_{gT} = 1 - \frac{H_L}{H_D} \tag{3}$$

The gas holdup in the gas–liquid separator was calculated from a gas volume balance:

$$E_{gT}V_{gT} = E_{gr}V_{gr} + E_{gd}V_{gd} + E_{gs}V_{gs} + E_{gb}V_{gb} \tag{4}$$

Neglecting the last term in the right-hand side in view of the small volume and very low gas holdup in the bottom section and taking into account the geometrical characteristics of the system, the separator holdup may be calculated from the equation [27]:

$$E_{gs} = \frac{(E_{gT}V_{LT}/(1 - E_{gT})) - E_{gr}H_rA_r - E_{gd}H_dA_d}{(V_{LT}/(1 - E_{gT})) - H_r(A_r - A_d) - h_bA_b} \tag{5}$$

2.4. Liquid circulation velocity

Liquid circulation velocity was determined by a signal-response technique using HCl acid tracer and a pH electrode detector [28–31]. In this work, four pH electrodes, two located in the riser and two in the downcomer sections were used. The response time of the pH electrodes was 0.1 s. The response of a pulse input of the tracer was signaled by the pH electrodes, and monitored by a pH meter (sensitivity: 0.01), respectively, and then simultaneously recorded every 5 s on a chart and a digital printer. The chart recording was synchronized manually with the introduction of every pulse of 10 mL 4 M (4N) HCL solution through the injection port. For the pH measurements in the riser section, the bottom port was used as the tracer injection port. The top port was used as tracer injection port during pH measurements in the downcomer section.

A typical response curve of pH against time obtained by the pH electrodes is shown in Fig. 2. The measured pH values of the liquid in the riser and the downcomer sections were then converted to the actual concentrations through a calibration curve.

The mean circulation time, t_C (time for a liquid volume element to travel once around the riser–downcomer circuit) was determined directly from the response curves observed for each airflow rate. The number of cycles detectable varied with the airflow rate. At low airflow rate, the number of cycles was six but at the highest airflow rate it was only a few. Therefore, experiments conducted at high-airflow rates were duplicated to obtain more reliable values for t_C.

With the mean circulation time t_C, the liquid linear and superficial velocities in the riser and downcomer were estimated using the following equations:

$$U_{Lr} = \frac{z_r(1 - E_{gr})}{\Delta t_r} \tag{6}$$

$$U_{Ld} = \frac{z_d(1 - E_{gd})}{\Delta t_d} \tag{7}$$

where z_r and z_d are the distances between the two pH electrodes in the riser and downcomer, respectively, and Δt_r and Δt_d are the average differences in response time of the second and third peaks of the response curves obtained by the two pH electrodes in the riser and downcomer, respectively. Note that the second and the third peaks of the response curves are used to obtain Δt_r and Δt_d because the first peak of the response curve obtained by the lower pH electrode in the riser is not well-established at higher aeration rate [5].

3. Results and discussion

3.1. Gas holdup

Fig. 3 describes the effect of the bottom clearance on riser and downcomer gas holdups for the air–water system. The gas holdup increases in the riser as the bottom clearance decreases. This can be understood as being caused by a decrease in the

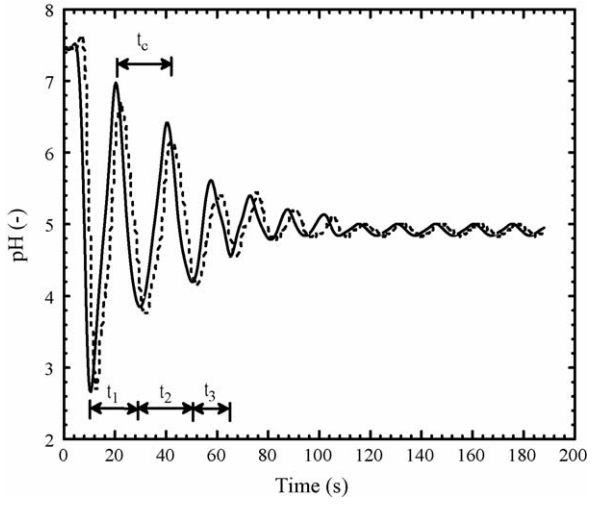

Fig. 2. Typical response curves measured using two pH electrode sensors, one located at the entrance and another at the exit of the riser or downcomer regions of the airlift reactors.

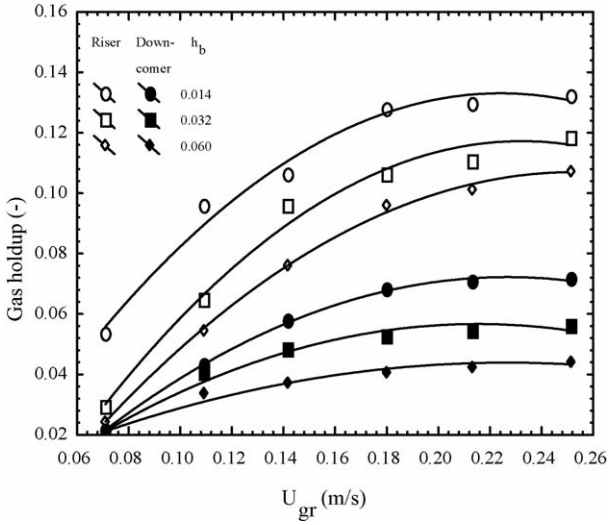

Fig. 3. Average riser and downcomer gas holdup for the bottom and top clearance of $h_t = 0.225$ m; air–water system.

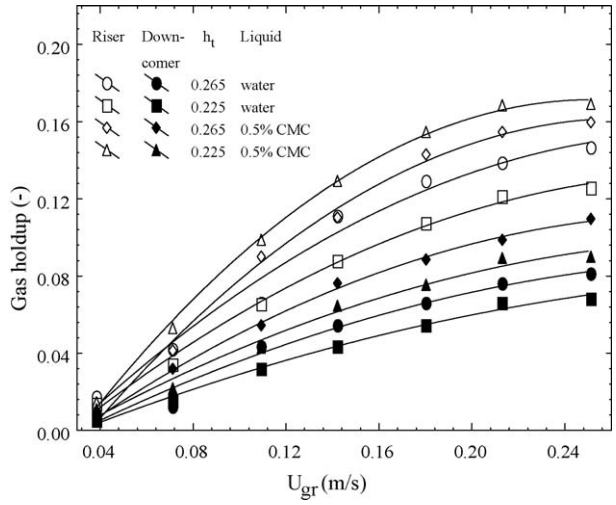

Fig. 4. Average riser and downcomer gas holdups for a bottom clearance of $h_b = 0.014$ m and top clearances of $h_t = 0.225$ and 0.265 m.

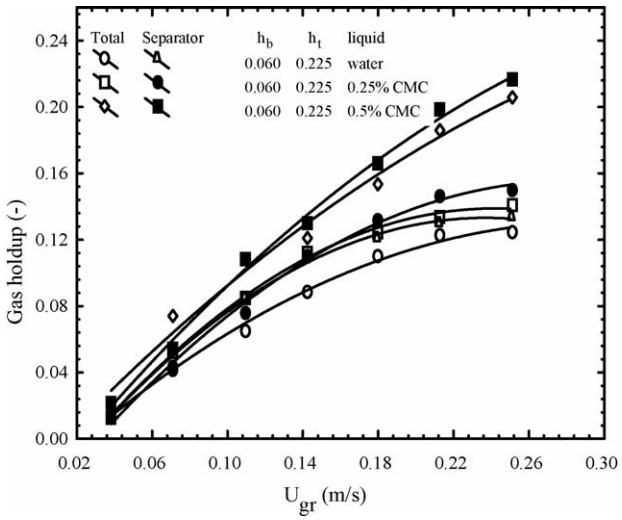

Fig. 5. Total and separator gas holdup for constant top and bottom clearances and three liquids.

liquid velocity. This is especially evident in the data for the downcomer gas holdup, since for the smallest bottom clearance the velocity of the liquid is so restricted by the pressure drop in the bottom of the reactor that almost all the gas disengages in the gas–liquid separator. The gas holdup in the downcomer is almost zero at low values of the superficial gas velocity U_{gr}.

Fig. 4 shows the gas holdup in the riser and downcomer, for a bottom clearance of 0.014 m and two values of the top clearance: $h_t = 0.225$ and 0.265 m. Data are presented for water and 0.15 M NaCl–0.5% CMC solution. While for water h_t has a small effect, this is not so for the more viscous mineralized CMC solution. In the latter, the lower rising velocity of the bubbles causes more of them to be entrained and carried down by the liquid, and therefore the larger residence time in the gas–liquid separator region due to the larger bubbles that recirculate.

The lower h_t gives a shorter residence time in the gas–liquid separator, a larger bubble recirculation, and, therefore, a larger gas holdup. This is especially evident in the downcomer for the mineralized viscous CMC solution.

The measured total and separator gas holdups are shown in Fig. 5 as a function of the superficial gas velocity U_{gr} for different liquids and constant values of the bottom and top clearances. Fig. 6 shows separator gas holdup as a function of the superficial gas velocity U_{gr} for various values of the bottom and top clearances. It is interesting to note that the separator gas holdup is essentially the same for $h_b = 0.032$ and 0.060 m (cf., Fig. 6), indicating balancing of the decrease of E_r by an increase of E_d as the liquid velocity increases. The separator gas holdup (E_s) was higher for the 0.25% and 0.5% NaCl–CMC solution than for water, especially at high U_{gr}. This is due to the lower bubble disengagement, which in turn results from the lower rising velocity in the mineralized viscous CMC solution. The separator gas holdup behaves generally as the total gas holdup (E_T) (cf., Fig. 5). Comparing Figs. 3 and 4 one can see the effects of the expanded gas–liquid separator. All the data indicates that disengagement was more effective in the rectangular airlift reactor proposed in this study. This indicates that the cross-sectional area of the gas separator has a strong influence on the fluid dynamics of the reactor. This was shown by the regression analysis, which is presented in Section 3.2.

3.2. Liquid circulation velocity

Fig. 7 shows the liquid velocity evolution versus the superficial gas velocity in the riser and the influence of the top clearance h_t on U_{Lr}. U_{Lr} increases with U_{gr} until $U_{gr} \approx 0.21\ m\ s^{-1}$, and then reaches a plateau value for $U_{gr} > 0.21\ m\ s^{-1}$. In our reactor configuration, gas bubbles were trapped in the downcomer and therefore, U_{Lr} reached a plateau. Couvert et al. [6] and Livingston and Zhang [32] observed the same phenomenon. However, in their cases, the plateau was obtained for $U_{gr} > 0.015\ m\ s^{-1}$ and $U_{gr} > 0.02$–$0.03\ m\ s^{-1}$, respectively.

Fig. 8 shows a small but distinct influence of the baffle bottom clearance on the superficial riser liquid. The liquid velocity increases to a maximum with increasing h_b in the range

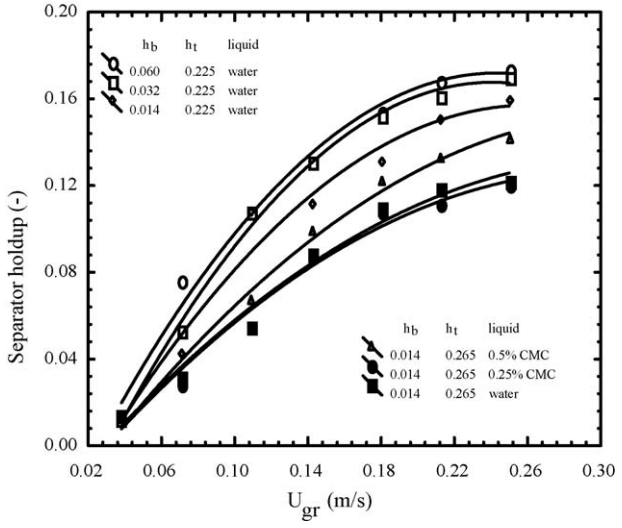

Fig. 6. Separator gas holdup for various top and bottom clearances and three liquids.

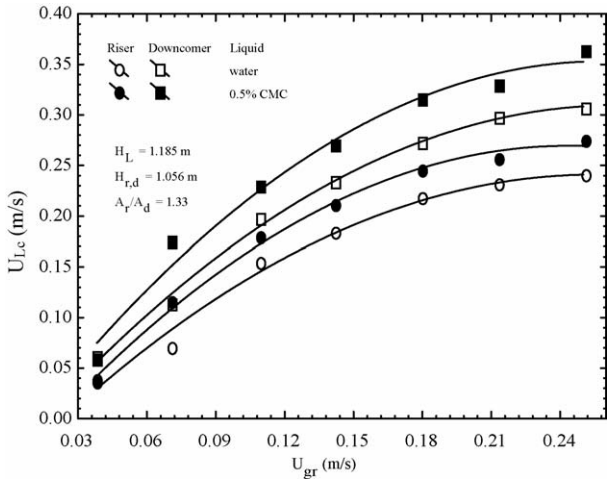

Fig. 7. Influence of the gas superficial velocity on riser and downcomer liquid velocities, for $h_t = 0.265$ m and $h_b = 0.060$ m and two liquids (water, 0.15 M NaCl–0.5% CMC solution).

$h_b < 0.076$ m (or $h_b/D_{hr} = 0.86$) and again diminishes with further increase of h_b. Kochbeck and Hempel [12] and Bando et al. [10,11,33] observed the same trend. However, these results differed slightly with those reported in this work and by Koide et al. [13].

Fig. 9 shows the effect of h_t on U_{Lr} for the air–water system. The liquid circulation velocity increases with increasing h_t, and becomes unchanged when h_t is beyond a critical value $h_{t,crt} = 0.175$ m for the column hydraulic diameter of $D_{hc} = 0.10$ m. The flow resistance to the reverse direction in the region above the upper end of the baffles is large at relatively short h_t and it decreases with increasing h_t. When h_t is beyond the critical value, the flow resistance becomes constant. From Fig. 9, it is considered that the critical value of h_t is a function of the column diameter and independent of the diameter and length of the riser, gas velocity and bubble size (d_B).

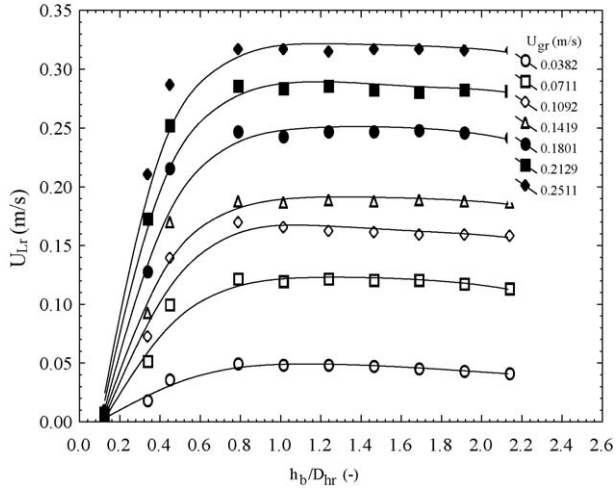

Fig. 8. Plot of liquid circulations velocity against difference in gas holdups between the riser and the downcomer for air–water system and $h_b = 0.265$ m at various gas superficial velocities and top clearances.

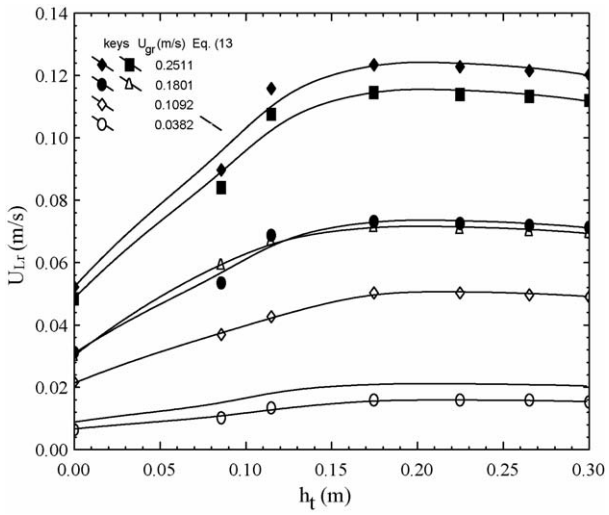

Fig. 9. Effect of h_t on U_{Lr} for the air–water system and $h_b = 0.265$ m at various gas superficial velocities.

4. Correlation of the experimental results

4.1. Gas holdup

Merchuk et al. [7] and Koide et al. [13,14] obtained semi-empirical correlations for gas holdups in an internal loop airlift reactor using water and CMC solutions. On the basis of their information, the following correlations were obtained from 56 data points to predict the gas holdup for each hydrodynamic region of the ALR proposed in this study.

Correlation ($R = 0.998$; $R^2 = 0.996$; S.D. = 0.075; S.T.D. error = 0.0078) for riser gas holdup E_r:

$$E_r = 770\left(\frac{U_{gr}}{\sqrt{gD_{hc}}}\right)^{1.621}\left(\frac{g\eta_L^4}{\rho_L\sigma_L^3}\right)^{0.852}\left(\frac{h_b}{D_{hr}}\right)^{0.180} \times\left(\frac{D_{es}}{D_{hc}}\right)^{11.375}\left(\frac{h_t}{D_{hr}}\right)^{5.2} \quad (8)$$

Correlation ($R = 0.952$; $R^2 = 0.888$; S.D. = 0.051; S.T.D. error = 0.0037) for downcomer gas holdup E_d:

$$E_d = 570\left(\frac{U_{gr}}{\sqrt{gD_{hc}}}\right)^{2.82}\left(\frac{g\eta_L^4}{\rho_L\sigma_L^3}\right)^{0.968}\left(\frac{h_b}{D_{hr}}\right)^{0.210} \times\left(\frac{D_{hs}}{D_{hc}}\right)^{11.375}\left(\frac{g\rho_L^2 D_{hc}^3}{\eta_L^2}\right)^{0.2} \quad (9)$$

Correlation ($R = 0.997$, $R^2 = 0.993$; S.D. = 0.092; S.T.D. error = 0.0075) for total gas holdup E_s:

$$E_s = 800.5\left(\frac{U_{gr}}{\sqrt{gD_{hc}}}\right)^{1.73}\left(\frac{g\eta_L^4}{\rho_L\sigma_L^3}\right)^{0.852}\left(\frac{h_b}{D_{hr}}\right)^{0.08} \times\left(\frac{D_{hs}}{D_{hc}}\right)^{11.5}\left(\frac{h_t}{D_{hr}}\right)^{4.82} \quad (10)$$

with the correlation of riser gas holdup, Eq. (8). Correlations (8)–(10) which are based on data within the ranges:

$$\left.\begin{array}{l} \dfrac{0.0008 < (U_{gr})}{(\sqrt{gD_{hc}}) < 0.45} \\ \dfrac{2\times10^{8} < (g\rho_L^2 D_{ec}^3)}{\eta_L^2 < 8\times10^{15}} \\ \dfrac{4\times10^{5} < (g\eta_L^4)}{\rho_L\sigma_L^3 < 4\times10^{12}} \\ \dfrac{0.01 < h_b}{D_{hr} < 0.1} \\ \dfrac{0.1 < D_{hs}}{D_{hc} < 0.5} \\ 0.045 < \sigma_L < 0.085\,\text{N/m} \\ 0.02 < \eta_{eff} < 0.5\,\text{Pas} \\ 0.33\times10^{-9} < D_L < 2.55\times10^{-9}\,\text{m}^2/\text{s} \end{array}\right\} \quad (11)$$

Eq. (10) is valid also for the total gas holdup E_T.

Fig. 10 compares the present and the reported data and reveals the roles played by the different regions in the rectangular airlift reactor. The relative contribution of the riser and downcomer to the separator and/or total gas holdups are different and complementary. The main term $((U_{gr})/(gD_{hc})^{0.5})$, which represents the influence of gas input rate and the liquid circulation rate, affects the holdup more strongly in the downcomer than in the riser. The behavior of the gas holdup in the gas separator is very close to that of the total gas holdup (Fig. 3). The bottom clearance, represented by the term (h_b/D_{hr}), exerts its influence on the gas holdup in all the regions. The exponent of $[h_b/D_{hr}]$ is positive in all the regions, indicating the effect of the liquid velocity. As h_b increases, the liquid circulation increases as well, and more gas bubbles are carried over into the downcomer. The exponent 0.21 on $[h_b/D_{hr}]$ in Eq. (9) indicates that E_d could be increased up to two-fold by changing the bottom clearance within the range of variables ($U_{gr} = 0.0382 - 0.2511\,\text{m s}^{-1}$, $h_b = 0.014 - 0.094\,\text{m}$) tested.

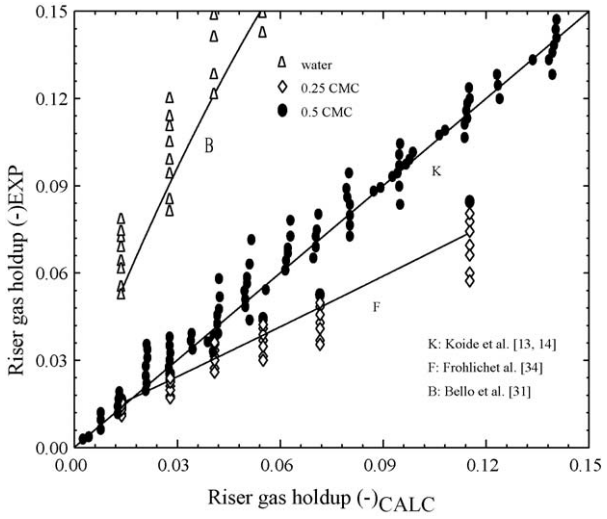

Fig. 10. Parity plot of experimentally obtained values of the riser holdup vs. those calculated from Eq. (8) and comparison with data and correlations previously published.

The effect of the top clearance, represented by the group $[h_t/D_{hr}]$, had a large influence on the riser and separator gas holdup, but none on the downcomer gas holdup. An increase in the top clearance decreases the gas holdup. The correlations show that the viscosity (η_L) and surface tension (σ_L), have a significant influence on gas holdups for the liquids tested and within the range of the variables inspected. They do significantly affect the downcomer gas holdup, because of the strong influence of free rising velocity of the bubbles ($U_{B\infty}$) on the bubble entrainment. A smaller influence is detected in the riser and separator gas holdup than in the downcomer. This is due to the fact that the downcomer holdup is smaller than in the riser and separator regions of the reactor. The dimensional groups $[(g\rho_L^2 D_{hc}^3)/(\eta_L^2)]$ and $[(g\eta_L^4)/(\rho_L\sigma_L^3)]$ do not show a statistically significant influence on the separator E_s gas holdup. At higher values of U_{gr} and the highest concentration of 0.15 M NaCl–CMC solution, considerably higher separator E_s gas holdup is observed (Fig. 5). This does not have much of an effect on $R^2 = 0.993$, but the correlation may underestimate the effect of viscosity and surface tension under the above conditions.

Fig. 10 shows data reported by Koide et al. [13,14]. These correlations fit those data satisfactorily. The data reported by Bello et al. [31] are also well represented by Eq. (10). In addition to these experimental data, Fig. 10 also shows the correlation by Frohlich et al. [34]. This correlation deviates slightly from the one presented here. It should also be noted that the Frohlich correlation requires the liquid velocity as an argument. In the present work, we took the velocity corresponding to the largest value of h_b, which is closer to the range of variables taken by Frohlich et al. [34].

4.2. Liquid circulation velocity

Lu et al. [16] and Bello et al. [31], correlated the liquid velocity as $U_{Lr} = \alpha(A_d/A_r)^{\beta}\ (U_{gr})^{\delta}(1 - E_r)$ with α, β, and $\delta = 0.124$, 0.08, 0.537 and 0.66, 0.78 ± 0.08, 0.33 for rectangular and concentric airlift reactors, respectively. Kockbeck and Hempel [12] correlated the liquid velocity as $U_{Lr} = (2gH_{r,d}E_r/[f_b(A_d/A_r)^2])^{1/2}$ with $f_b = 11.402\ (A_d/A_b)^y$ where $y = 0.789$. Fig. 11 shows that this correction cannot be applied for the investigated reactor configuration. In the present configuration, some bubbles are entrained and trapped in the downcomer and therefore, U_{Lr} reaches a plateau. The experimental and calculated values differ by up to ±29%.

The pressure balance over the reactor gives an explanation for the above mentioned discrepancies. The liquid flow in the investigated rectangular airlift loop reactor was based on the pressure difference (ΔP_{hydro}) between the riser and the downcomer.

$$\Delta P_{hydro} = \rho_L g H_{r,d}(E_{gr} - E_{gd}) \quad (12)$$

The hydrostatic pressure is balanced by the dynamic pressure drop (ΔP_{dyn}, Eq. (13)), which is the sum of the pressure drops in the riser (ΔP_r), downcomer (ΔP_d), bottom (ΔP_b), and top

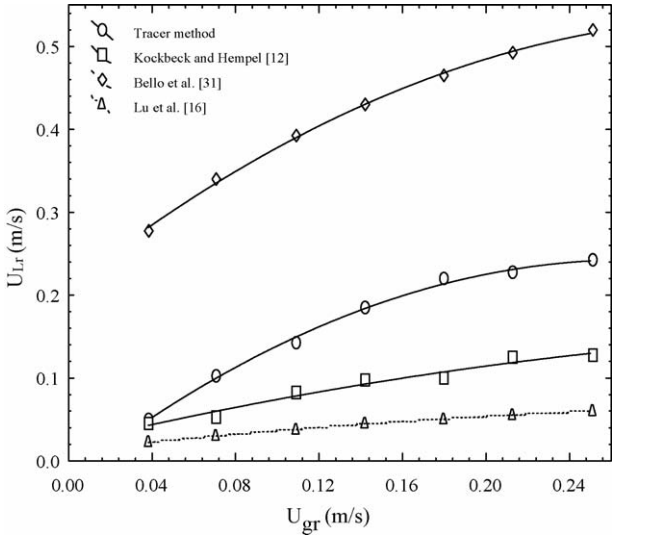

Fig. 11. Bulk liquid velocity vs. U_{gr} for $h_t = 0.265$ m and $h_b = 0.060$ m and air–water system.

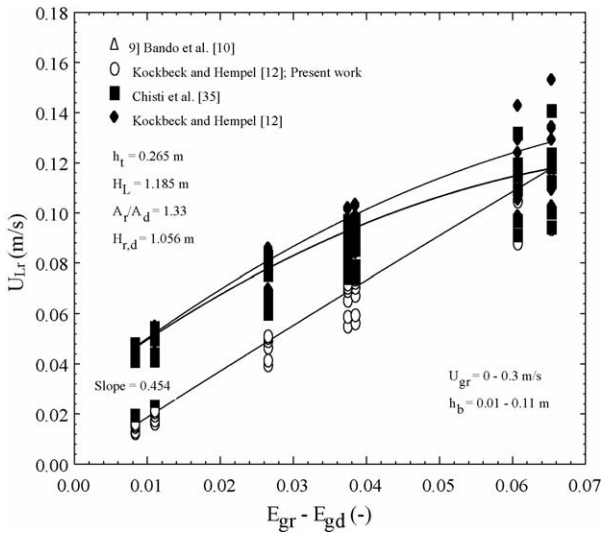

Fig. 12. Effect of h_b on U_{Lr} for air–water system and $h_t = 0.265$ m at various gas superficial velocities.

(ΔP_t) regions of the reactor (cf., Fig. 1).

$$\Delta P_{dyn} = \Delta P_r + \Delta P_d + \Delta P_b + \Delta P_t \tag{13}$$

The details of the derivation of the final U_{Lr} (Eq. (14)) leading from Eqs. (12) and (13) are found elsewhere [12]. Eq. (14) is a modified version of the one presented by Kockbeck and Hempel [12], where f_t and f_b are the loss coefficients in the regions above the upper end of the baffles, respectively. Chisti et al. [35] have correlated f_b with the column bottom configuration.

$$U_{Lr} = \left[\frac{2gH_{r,d}(E_{gr} - E_{gd})}{f_r + f_t(2A_r/A_r + (A_r - A_d)[1 - (E_{gs} + E_{gr})])^2 + f_b(2A_r/A_d + (A_r - A_d)[1 - (E_{gr} + E_{gd})])^2} \right]^{0.5} \tag{14}$$

$$f_b = 11.402\left(\frac{A_d}{A_b}\right)^{0.789} \tag{15}$$

Bando et al. [10] correlated f_t with riser, top clearance and column configurations using the following equations:

$$f_t = 10\left(\frac{D_{hr}}{D_{hc}}\right)^{-5.6} \exp\left(-\frac{1.7h_t}{D_{hc}}\right), \quad \frac{h_t}{D_{hc}} < 2 \tag{16}$$

and

$$f_t = 0.33\left(\frac{D_{hr}}{D_{hc}}\right)^{-5.6}, \quad \frac{h_t}{D_{hc}} > 2 \tag{17}$$

where A_d and A_b are cross-sectional areas of downcomer and bottom free zone between the riser and the downcomer. D_{hr} and D_{hc} are the equivalent hydraulic diameters of the riser and column, respectively. In the present study:

$$A_b = W_d h_b, \quad A_d = W_d L_d \tag{18}$$

where h_b is considered constant and equal to 0.095 m, f_b equals to 43 and is constant also for all experimental conditions. From Eqs. (14)–(17), when f_t is constant, the liquid circulation velocity is regarded to be proportional to the square root of the gas holdup difference between the riser and the downcomer ($\Delta E_g = E_{gr} - E_{gd}$) and vice versa.

Figs. 12 and 13 shows the effect of bottom and top clearances, respectively, on liquid circulation velocity plotted against the gas holdup difference between riser and downcomer for the data observed in previous works [10,12,35] and in this work. The U_{Lr} observed by Kockbeck and Hempel [12] ($h_b = 0.04 - 0.20$ m, $A_r/A_d = 6.4 - 17.4$) roughly agree with those observed in this work. When the gas velocity is variable under constant h_t, the liquid circulation velocity is roughly linear to the square root of the gas holdup difference. On the other hand, when h_t and h_b are variable under the constant gas velocity, the data hardly ride on the lines with slope of 0.454 (Fig. 12) and 0.115 (Fig. 13), respectively. From this, the loss coefficients are considered to change due to the variable h_t and h_b.

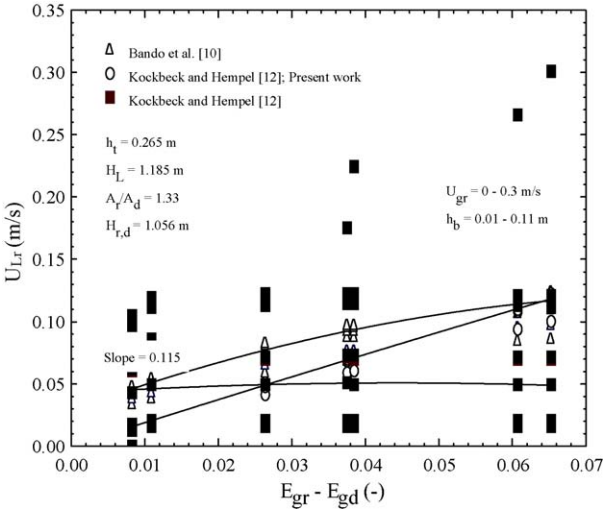

Fig. 13. Effect of h_t on U_{Lr} for air–water system and $h_b = 0.095$ m at various gas superficial velocities.

5. Conclusions

Experiments have been carried out using water and mineralized CMC solutions of effective viscosity ranging from 0.02 to 0.5 Pa s, and surface tension from 0.065 to 0.085 N/m to investigate the influence of baffle (top and bottom) clearance design on gas holdup and liquid circulation velocity in a two riser rectangular airlift reactor with inverse internal loop and expanded gas–liquid separator. The gas holdups for each of the different hydrodynamic regions in the rectangular airlift reactor: riser, downcomer, and gas–liquid separator were successfully correlated using expressions derived through dimensional analysis for several bottom and top clearances.

The experimental results for the liquid circulation velocity were successfully correlated using empirical models obtained via pressure balance and loss coefficient. The calculated and measured values agreed within an error of ±29%. The liquid circulation velocity increased when the top and bottom clearances were increased and remained unchanged when h_b/D_{hr} and h_t were above 1.0 and 0.175 m, respectively. Both the bottom and top baffle clearances were found to influence liquid velocity to some degree. The bottom clearance was considered the most important characteristic.

The liquid circulation velocity data revealed that the design of the gas–liquid separator is a very important factor affecting the hydrodynamic performance. This has been already stated earlier by other investigators (Freitas and Teixeira [36], Siegel and Merchuk [37], and Vicent and Teixeira [38].

Acknowledgements

We acknowledge the support by the Ontario Government Scholarship (OGS) awarded to Peter M. Kilonzo and the support by the Natural Science and Engineering Research Council of Canada (NSERC) awarded to Dr. A. Margaritis through individual Discovery Grants.

Appendix A. Calculation of coefficients

The experimentally measured data for the liquid velocities and gas holdups for the double riser rectangular airlift reactor with inverse internal-loop and expanded gas–liquid separator were correlated with the equation developed by [35]:

$$U_{Lr} = \left[\frac{2gH_{r,d}(E_{gr} - E_{gd})}{f_t'/(1-E_{gr})^2 + f_b'(A_r/A_d)^2(1/(1-E_{gd})^2)}\right]^{1/2} \quad (A1)$$

Note that Eq. (A1) contains both f_b and f_t because the connections of the riser and downcomer at the top and bottom sections were assumed to have different geometries. The values of f_b' and f_t' required to achieve best fit of the data with Eq. (A1) were calculated using the reactor geometry. The calculated f_b values were correlated with the geometric variables as using the equation:

$$P_{Tr} - P_{Td} = \frac{1}{2}\rho_L U_{Lr}^2 f_{tE} + \frac{1}{2} f_{tC}\rho_L U_{Ld}^2 \quad (A2)$$

For the simulations reported in this work, the geometrical dependent frictional loss coefficient at the top section was evaluated equal to $f_{tC} = 14.06$. The calculated value was due to the fluid expansion from the riser region to the gas separation region f_{tE} and fluid contraction from the separator to the downcomer region f_{tC}. Their calculated values $f_{tE} = 0.82$ for the geometric variables (A_r/A_t) was correlated with the empirical Eq. (A3) [39,40]

$$f_{tE} = \left[1 - \left(\frac{A_r}{A_s}\right)\right]^2 \quad (A3)$$

while $f_{tC} = 13.24$ was correlated with the geometric variables (A_t/A_d) [41,42] using the equation

$$f_{tC} = \left(\frac{A_s}{A_d} - 1\right) \quad (A4)$$

where A_t is the cross-sectional area of the liquid level in the gas–liquid separator. The total top frictional coefficient was evaluated as a sum of the expansion and contraction terms at the top section as:

$$f_t = f_{tE} + f_{tC} \quad (A5)$$

A high value of 54.52 was used for the bottom loss coefficient f_b to simulate the restricted flow situation to account for the pressure drop through the gap between the baffle bottom and the base plate f_b and through the sparger system f_{bSP}. The value of $f_b' = 17.66$ account for fluid contraction from the downcomer to the riser and was evaluated for the geometric ratio $A_d/A_b = 0.72$ having the bottom clearance $h_b = 0.06$ m. The calculated value was correlated with the empirical equation [5,43,44]

$$f_b' = 11.402\left(\frac{A_d}{A_b}\right)^{0.789} \quad (A6)$$

where A_b is the free cross-sectional area of fluid flow at the bottom of the baffle.

A value of $f_{bSP} = 36.86$ was obtained to account for the fluid contraction through the sparger tube system from the bottom of the riser having the geometric $A_r/A_{FSP} = 1.84$, and correlated with the equation:

$$f_{bSP} = 11.402\left(\frac{A_r}{A_{FSP}}\right)^{0.789} \quad (A7)$$

where A_{FSP} is the free area of flow in the sparging regions, given by the equation:

$$A_{FSP} = A_r - A_{SP} \quad (A8)$$

The overall bottom coefficient f_b is the sum of the two coefficients accounting for the restricted flow through the baffle bottom f_b', and sparger tubes f_{bSP}, i.e.,

$$f_b = f_b' + f_{bSP} \quad (A9)$$

References

[1] Y. Chisti, Airlift Bioreactors, Elsevier, London/New York, 1989.
[2] U. Onken, P. Weiland, Airlift fermenters: construction behaviour and uses, in: Adv. Biotechnol. Proc., vol. 1, Alan R. Liss, New York, 1983.

[3] Y. Chisti, M. Moo-Young, Airlift bioreactorts for treatment of hydrocarbon contaminated wastes, in: W.K. Teo, M.G.S. Yap, S.K.W. Oh (Eds.), Better Living through Biochemical Engineering, University of Singapore, Singapore, 1999.
[4] P. Varey, Airlift for purity, Chemical Eng. (London) 529 (1992) 37.
[5] W.-J. Lu, S.-J. Hwang, C.-M. Chang, Liquid velocity and gas holdup in three-phase internal loop airlift reactors, Chem. Eng. Sci. 30 (1995) 1301–1310.
[6] A. Couvert, M. Roustan, P. Chatellier, Two-phase hydrodynamic study in a rectangular air-lift loop reactor with an internal baffle, Chem. Eng. Sci. 54 (1999) 5245–5252.
[7] J.C. Merchuk, N. Ladwa, A. Cameron, M. Bulmer, A. Picket, Concentric-tube airlift reactors: Effects of geometrical design on performance, AIChE J. 40 (1994) 1105–1117.
[8] V. Lazarova, J. Meyniel, L. Duval, J. Manem, A novel circulating bed reactor: hydrodynamics, mass transfer and nitrification capacity, Chem. Eng. Sci. 52 (1997) 3919–3927.
[9] F. Yamashita, Gas holdup in bubble column with draft tube for gas dispersion annulus, Chem. Eng. Jpn. 31 (2) (1998) 289–294.
[10] Y. Bando, K. Fujimori, H. Terazawa, K. Yasuda, M. Nakamura, Effects of equipment dimensions on circulation flow rates of liquid and gas in bubble column with draft tube, J. Chem. Eng. Jpn. 33 (3) (2000) 379–385.
[11] Y. Bando, H. Hayakawa, M. Nakamura, Effects of equipment dimensions on liquid mixing time of bubble column with draft tube, J. Chem. Eng. Jpn. 31 (5) (1998) 765–770.
[12] B. Kochbech, D.C. Hempel, Liquid velocity and dispersion coefficient in an airlift reactor with inverse internal loop, Chem. Eng. Technol. 17 (1994) 401–405.
[13] K. Koide, M. Kimura, H. Nitta, H. Kawabata, Liquid circulation in bubble column with draught tube, J. Chem. Eng. Jpn. 21 (4) (1988) 393–399.
[14] K. Koide, S. Iwamoto, T. Takasaka, S. Matsuura, E. Takahashi, M. Kimura, H. Kubota, Liquid Circulation, Gas holdup and pressure drop in bubble column with draft tube, J. Chem. Eng. Jpn. 17 (6) (1984) 611–618.
[15] K. Koide, H. Sato, H. Iwamoto, Gas holdup and volumetric liquid phase mass transfer coefficient in bubble column with draft tube and with gas dispersion into annulus, J. Chem. Eng. Jpn. 16 (1983) 407–413.
[16] X. Lu, J. Ding, Y. Wang, J. Shi, Comparison of hydrodynamics and mass transfer characteristics, of a modified square airlift reactor with common airlift reactors, Chem. Eng. Sci. 55 (2000) 2257–2263.
[17] P.-M. Wang, T.-K. Huang, H.-P. Cheng, Y.-H. Chien, W.-T. Wu, A modified airlift reactor with high capabilities of liquid mixing and mass transfer, J. Chem. Eng. Jpn. 35 (2002) 354–359.
[18] P.M. Kilonzo, A. Margaritis, The effect of non-Newtonian fermentation broth viscosity and small bubble segregation on oxygen mass transfer in gas-lift bioreactors: a critical review, Biochem. Eng. J. 17 (2004) 27–40.
[19] E.E. Petersen, A. Margaritis, Hydrodynamic and mass transfer characteristic of three-phase gaslift bioreactor systems, Crit. Rev. Biotechnol. 21 (4) (2001) 233–294.
[20] M.K. Popovic, C.W. Robinson, Mass transfer studies of external-loop airlifts and bubble column, AIChE J. 35 (1989) 393–405.
[21] P. Shamlou, D.J. Pollard, A.P. Ison, M.D. Lilly, Gas holdup and liquid circulation rate in concentric tube airlift bioreactors, Chem. Eng. Sci. 49 (3) (1994) 303–312.
[22] M. Nishikawa, H. Kato, K. Hashimoto, Heat transfer in aerated tower filled with non-Newtonian liquids, Ind. Eng. Proc. Des. Dev. 16 (1977) 133–137.
[23] M. Nakanoh, F. Yoshida, Gas absorption by Newtonian and non-Newtonian liquids in a bubble column, Ind. Eng. Chem. Process Des. Dev. 19 (1980) 190–195.
[24] D.G. Allen, C.W. Robinson, Hydrodynamics and mass transfer in *Aspergillus niger* fermentations in bubble column and loop bioreactors, Biotechnol. Bioeng. 34 (1989) 731–740.
[25] G.G. Li, S.-Z. Yang, Z.-L. Cai, J.-Y. Chen, Mass transfer and gas–liquid circulation in an airlift bioreactor with viscous non-Newtonian fluids, Chem. Eng. J. 56 (1995) B101–B107.
[26] M. Moo-Young, B. Hallard, D.G. Allen, R. Rurrel, Y. Kawase, Oxygen transfer to mycelial fermentation broths in an airlift fermenter, Biotechnol. Bioeng. 30 (1987) 746–753.
[27] C. Vial, E. Camarasa, S. Poncin, G. Wild, N. Midoux, J. Bouillard, Study of hydrodynamic behavior in bubble columns and external loop airlift reactors through analysis of pressure fluctuations, Chem. Eng. Sci. 55 (2000) 2957–2973.
[28] A.B. Russe, C.R. Thomas, M.D. Lilly, The influence of height and top-section size on the hydrodynamic characteristics of airlift fomenters, Biotechnol. Bioeng. 43 (1994) 69–76.
[29] Y. Kawase, N. Omori, M. Tsujimura, Liquid–phase mixing in external-loop bioreactors, Chem. Technol. Biotechnol. 63 (1994) 49–55.
[30] Y. Wang, B. McNeil, A study of gas holdup, liquid velocity, and mixing time in a complex high viscosity, fermentation fluid in an airlift bioreactor, Chem. Eng. Technol. 19 (1996) 143–153.
[31] R.A. Bello, C.W. Robinson, M. Moo-Young, Liquid circulation and mixing characteristics of airlift contactors, Can. J. Chem. Eng. 62 (1984) 573–577.
[32] A.G. Livingston, S.F. Zhang, Hydrodynamic behavior of three-phase (gas–liquid–solid) gaslift reactors, Chem. Eng. Sci. 48 (1993) 1641–1654.
[33] Y. Bando, M. Nakamura, H. Sota, K. Toyoda, S. Sizuki, A. Idota, Flow characteristics of bubble column with perforated draft tube—effect of equipment dimensions and gas dispersion, J. Chem. Eng. Jpn. 25 (1) (1992) 49–54.
[34] S. Frohlich, M. Lotz, T. Korte, A. Lubbert, K. Schugerl, M. Seekamp, Characterization of a pilot plant airlift tower loop bioreactor. I. Evaluation of the two-phase properties with model media, Biotechnol. Bioeng. 38 (1991) 43–45.
[35] M.Y. Chisti, B. Hallard, M. Moo-Young, Liquid circulation in airlift reactors, Chem. Eng. Sci. 43 (3) (1988) 451–457.
[36] C. Freitas, J.A. Teixeira, Hydrodynamic studies in an airlift reactor with enlarged degassing zone, Bioprocess. Eng. 18 (1998) 267–279.
[37] M. Siegel, J.C. Merchuk, Hydrodynamics in rectangular airlift reactors, scale-up and the influence of gas–liquid separator design, Can. J. Chem. Eng. 69 (1991) 465–473.
[38] A.A. Vicent, J.A. Teixeira, Hydrodynamic performance of three-phase airlift bioreactors with enlarged degassing zone, Bioprocess. Eng. 14 (1995) 17–22.
[39] M.A. Young, R.G. Carbonell, D.F. Ollis, Airlift Bioreactors: analysis of local two-phase hydrodynamics, AIChE J. 37 (3) (1991) 403–428.
[40] N. de Nevers, Fluid Mechanics for Chemical Engineers, McGraw-Hill, Inc., New York, 1991.
[41] P. Verlaan, J. Tramper, K. VanT Riet, A hydrodynamic model for an airlift-loop bioreator with external loop, Chem. Eng. J. 33 (1986) B43–B53.
[42] L.-S. Fan, S.-J. Hwang, A. Matsuura, Hydrodynamic behavior of a draft tube gas–liquid–solid spouted bed, Chem. Eng. Sci. 39 (12) (1984) 1677–1688.
[43] Y. Chisti, M. Moo-Young, Improve the performance of airlift reactors, Chem. Eng. Prog. 89 (1993) 38–45.
[44] Y. Chisti, M. Moo-Young, Communication to the editor on the calculation of shear rate and apparent viscosity in airlift and bubble column bioreactors, Biotechnol. Bioeng. 34 (1989) 1391–1392.